Applied Soil Ecology 213 (2025) 106313

Contents lists available at ScienceDirect

Applied Soil Ecology

journal homepage: www.elsevier.com/locate/apsoil

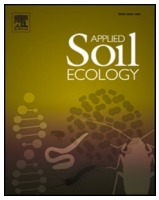

Research paper

# Soil functions are shaped by aridity through soil properties and the microbial community structure

Anna Doménech-Pascual [a,*], Luciana Chavez Rodriguez [b,c], Xingguo Han [d], Joan Pere Casas-Ruiz [a], Joan Ferriol-Ciurana [a], Jonathan Donhauser [e], Karen Jordaan [f], Steven D. Allison [b,g], Aline Frossard [d], Anders Priemé [e,h], Jean-Baptiste Ramond [f,i], Anna M. Romaní [a]

[a] GRECO, Institute of Aquatic Ecology, University of Girona, Spain
[b] Department of Ecology and Evolutionary Biology, University of California Irvine, USA
[c] Soil Biology Group, Wageningen University & Research, Wageningen, Gelderland, the Netherlands
[d] Swiss Federal Institute for Forest, Snow and Landscape Research, WSL, Switzerland
[e] Department of Biology, University of Copenhagen, Denmark
[f] Center for Microbial Ecology and Genomics, Department of Biochemistry, Genetics and Microbiology, University of Pretoria, South Africa
[g] Department of Earth System Science, University of California Irvine, USA
[h] Center for Volatile Interactions (VOLT), University of Copenhagen, Denmark
[i] Extreme Ecosystem Microbiomics and Ecogenomics laboratory, Biological Sciences Faculty, Pontificia Universidad Católica de Chile, Chile

ARTICLE INFO

*Keywords:*
Soil functions
Aridity gradient
Extracellular enzyme activities
Microbial biomass
Microbial respiration
Microbial community structure

ABSTRACT

Increasing aridity poses a threat to soil functionality, as it affects the key players -prokaryotes and fungi- responsible for these functions. Studying microbial diversity and functions in soils from different aridity conditions is crucial to understanding potential adaptations and response mechanisms to climate change, which may ultimately affect soil ecosystem multifunctionality. Here, we used a natural humid-to-arid climate gradient to determine: (1) if and how soil functions and microbial communities change across the aridity gradient; and (2) the main drivers of soil function variability along the gradient. We sampled soils (0–10 cm depth) from 12 sites across the Iberian Peninsula and analyzed their prokaryotic and fungal diversity and biomass as well as soil functions (aerobic respiration and extracellular enzyme activities linked to organic carbon, nitrogen and phosphorus degradation), together with soil physicochemical characteristics. Our results showed that increasing aridity resulted in a gradual change in the microbial community structure and a decrease in fungal diversity. However, soil functions did not show clear changes in response to aridity itself. Instead, microbial respiration and enzyme activities depended mainly on the local soil properties (i.e. organic matter quantity and quality, soil texture and pH) rather than on aridity. Overall, results indicated that in long-term climate-adapted soils, microbial functions are primarily driven by soil edaphology with aridity influencing them indirectly by shaping the microbial community composition and the intrinsic soil characteristics.

## 1. Introduction

Soil microorganisms are responsible for biogeochemical cycling and regulators of terrestrial ecosystem functions, playing a key role in maintaining ecosystem health and stability and accounting for 80–90 % of soil processes (Nannipieri et al., 2003). The sensitivity of soils to climate change, such as increasing aridity, may imply a reduction in soil functions, with a wide range of associated negative outcomes. Currently, approximately 40 % of all terrestrial ecosystems are drylands (Baker and Allison, 2017), which include sub-humid, semi-arid, arid and hyper-arid environments characterized by their high evapotranspiration potential and their low precipitation (aridity index values below 0.65) (Maier et al., 2018). Climate change observations and predictions suggest that drylands are expanding, together with increasing erratic and extreme weather events (Jansson and Hofmockel, 2020).

Aridity conditions shape soil microbial communities and their

* Corresponding author.
*E-mail addresses:* a.domenech@udg.edu, anna.domepas@gmail.com (A. Doménech-Pascual).

https://doi.org/10.1016/j.apsoil.2025.106313
Received 23 January 2025; Received in revised form 10 June 2025; Accepted 10 July 2025
Available online 16 July 2025

functions (Maestre et al., 2015; Schimel et al., 2007). Microorganisms have evolved strategies to adapt to aridity both at the cellular (e.g., spore formation, cell wall thickening or production and accumulation of osmolytes such as glycerol) (Gionchetta et al., 2020; Schimel, 2018), and community (e.g., biofilm formation, colonization of cryptic niches, compositional changes) levels (Makhalanyane et al., 2014). These two levels of adaptation are in turn intertwined. Changes in community structure to adapt to increasing aridity ultimately reflect differences in cellular level adaptations, whereby species with improved capacities to resist aridity replace the less resistant ones.

Although changes in microbial community composition due to different aridity have been observed in several studies (Maestre et al., 2015; Neilson et al., 2017; S. Wang et al., 2021), the impact of aridity on soil functions is not always apparent (Delgado-Baquerizo et al., 2016). This could be attributed to functional redundancy, in which different taxa can perform similar functions. Consequently, when taxa are lost due to increasing aridity, other remaining or newly introduced taxa can assume their roles (Louca et al., 2018; Nannipieri et al., 2003). However, it is generally observed that a decrease in soil water content negatively affects microbial respiration and soil multifunctionality (Durán et al., 2018; W. Liu et al., 2009). Additionally, drought conditions may result in a reduction of microbial activities involved in nutrient and carbon (C) cycling such as enzyme production (Delgado-Baquerizo et al., 2013), which can slow down organic matter decomposition rates (Durán et al., 2018).

Climate may also affect microbial communities and their functions through its effect on soil characteristics and vegetation. Climate change affects the precipitation regime, leading to modifications in the vegetation communities, which would impact the soil organic matter quality and availability of substrates for decomposers, consequently modifying prokaryotic and fungal biomass, community structure, and functionality (Védère et al., 2022). Furthermore, differences in climate are often correlated with differences in soil texture and pH, which are known to affect microbial diversity and function (Bastida et al., 2021; Dong et al., 2024; Eslaminejad et al., 2020). For example, increasing temperatures and decreasing moisture can lead to a reduction in soil pH (Zárate-Valdez et al., 2006), consequently impacting the biomass and the activity of microorganisms, such as their extracellular enzyme capabilities (Tale and Ingole, 2015; Zuccarini et al., 2023). Effects of soil geochemistry, including pH and soil organic C quality (e.g., C/N ratio) and quantity, on bacterial and fungal community structure and their function have also been reported (Fierer, 2017; Nouhra et al., 2018).

However, the final impact of these physicochemical parameters to soil microbes is not a simple addition of single effects but results from multiple interactions. For instance, in drylands, where soil pH tends to be high, microbial communities have exhibited greater resistance to pH fluctuations (Delgado-Baquerizo et al., 2020), possibly due to the buffering conditions provided by soils with a calcareous composition (Eslaminejad et al., 2020). Similarly, the respective relevance of silt and clay in enhancing soil organic matter content and in improving water holding capacity might be modified depending on the aridity conditions with potential contrasting effects to soil functions (Augustin and Cihacek, 2016). Given these multifactorial effects, many studies focus on short-term controlled experiments to isolate the effects of aridity. While these short-term studies are crucial and have provided relevant mechanistic knowledge (e.g., Schimel, 2018), field studies that include whole ecosystem interactions are needed to better understand adaptations of soil microbes in the long-term and decipher realistic functional responses to climate.

Here, we analyze soil prokaryotic and fungal community structure and a range of soil functions across a broad aridity gradient in the Iberian Peninsula. Our aim was to disentangle if and how aridity shapes soil microbial communities and functions related to organic matter cycling. Specifically, we aimed to: 1) study whether and how aridity shapes microbial community structure; 2) assess whether aridity shapes soil microbial functions (i.e. respiration and extracellular enzyme activities) and their link with community structure; and 3) determine the main drivers affecting functions along the aridity gradient. Our hypotheses were that: (i) aridity decreases microbial diversity and modifies community structure; (ii) soil functionality is negatively affected by increasing aridity; and (iii) climate and soil characteristics (such as pH and soil organic matter) are the main drivers of soil microbial functions. This study disentangles the interactions and relative relevance between climatic factors and soil characteristics in shaping microbial community structure and soil multifunctionality. Our findings provide insights into the long-term microbial adaptation to different climatic conditions, integrating the ecosystem-wide interactions that short-term studies may overlook.

## 2. Materials and methods

### 2.1. Study sites along the aridity gradient

Twelve sampling sites with different climates according to the Köppen classification were selected through the Iberian Peninsula, following an aridity gradient (Fig. 1). Land cover type classification was designated following the guide of Sulla-Menashe and Friedl (2018), and mapped using the data extracted with the Earth Data AppEEARS (NASA) software (AppEEARS Team, 2024) and the layers from the MODIS MCD12Q1 dataset (Friedl and Sulla-Menashe, 2019) (Fig. S1). Less arid sites are found at the north of Spain, with a temperate climate and no dry season (ATK, ARZ and VAL sites). Land cover in this zone is classified as deciduous broadleaf forest (Table 1). Sites with a temperate climate and dry summers are located at the northwest and northeast of the peninsula, in Galicia and Catalonia. They are differentiated by the presence of warm (LHE and FDE sites) or hot summers (GAV, MON, and ALB sites), respectively. Their vegetation is more diverse, consisting of deciduous broadleaf forests, evergreen needleleaf forests, mixed forests or open shrublands (Table 1). The most arid sites are located in the southeast and south of the peninsula, in Murcia and Almería (COY, SAN, MAL, and TAB sites), with a dry climate that can be semi-arid or arid hot or cold desert. They are open shrublands, grasslands, savannas and barren sites (Table 1). Climatic variables, i.e. mean annual temperature (MAT) and mean annual precipitation (MAP), are extracted from the worldclim database (https://worldclim.org/data/worldclim21.html), using a 30-year dataset and a 1 × 1 km resolution. The aridity Index (AI) was extracted from the dataset by Trabucco and Zomer (2022), which calculated AI as the ratio between precipitation and potential evapotranspiration (Zomer et al., 2022). AI ranges from 1.33 (less arid site) to 0.18 and 0.16 (Fig. 1, Table 1). To facilitate interpretation, aridity (1 - AI) is used for all analyses. MAT and MAP range from ~17 °C to 9–12 °C and from ~300 mm to 1300 mm, respectively (Table 1).

### 2.2. Soil sampling

The sampling campaign was performed during June and July 2021. At each site, five replicate soil samples were randomly collected from a sampling plot of 5 × 5 m. Each soil sample consisted of a surface soil core of 10 cm depth collected by PVC tubes (10 cm diameter). This sampling strategy resulted in the collection of a total of 60 individual soil samples. Soil cores were stored at 4 °C during the sampling campaign. Five replicates of surface litter (Litter, Table S1) were also collected from a 40 × 40 cm area at each site. A larger area of 60 × 60 cm was used at TAB and MAL due to the low litter accumulation at these sites. Litter subsamples were grinded (Retsch mixer mill, MM 400, Haan, Germany) for the total C and nitrogen (N) content (LTC, LTN, Table S1). At each sampling site, soil temperature (Table S1) was measured in-situ next to each core ($n$ = 5) with a soil thermometer every 15 min for one hour. Sampling hour for soil temperature recording was between 10:00 to 16:00, approximately.

At the lab, soils were sieved (4 mm mesh size) and subsamples for each analysis were separated. Enzyme activities, microbial respiration and water content were measured, within 7 to 10 days after collection.

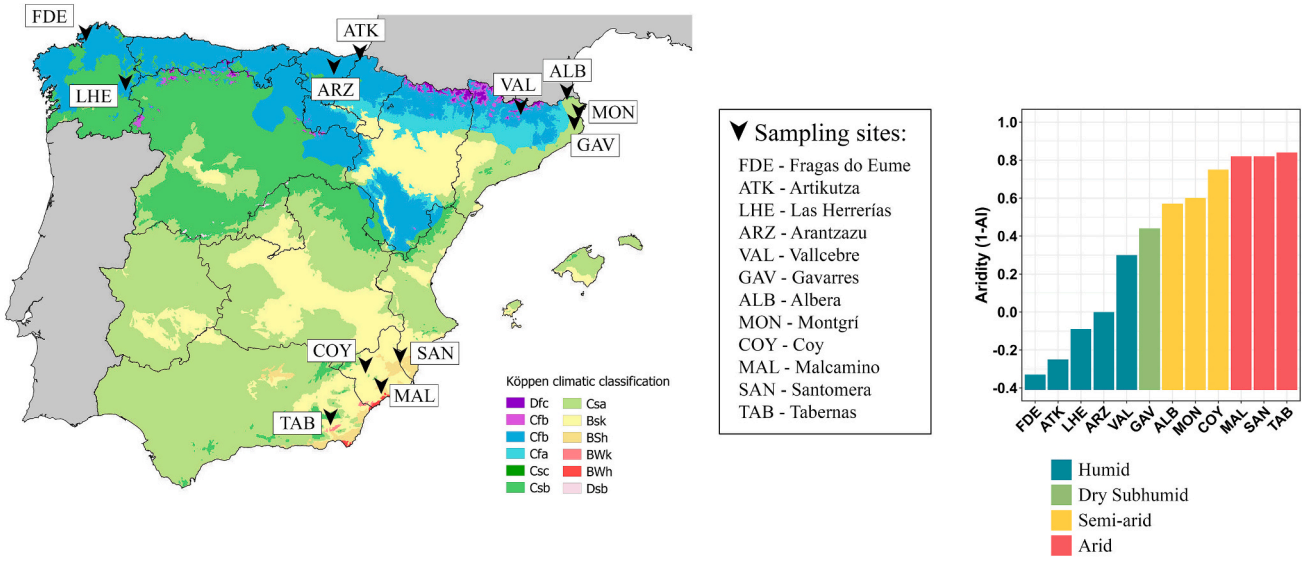


**Fig. 1.** Location of the 12 sampling sites in different Köppen climatic classification zones across Spain (left). Aridity, expressed as 1 - Aridity Index (AI), arranges the sites from the least (FDE) to the most arid (TAB) (right).

**Table 1**
Location of the sampling sites, their climate, land cover and soil characteristics. Climatic variables (AI, MAT and MAP) were extracted from the worldclim database (https://worldclim.org/data/worldclim21.html), using a 30-year dataset. AI = Aridity Index; MAT = Mean Annual Temperature; MAP = Mean Annual Precipitation. Landcover type classification was designated following the guide of Sulla-Menashe and Friedl (2018). Köppen classification abbreviations correspond to the following: Csb = Temperate, dry with warm summer; Cfb = Temperate, without dry season and with warm summer; Csa = Temperate, dry with hot summer; BSk = Dry semi-arid cold; BSh = Dry semi-arid hot; BWh = Dry arid hot.

| Site codes | Site name | Coordinates | Köppen | AI | MAT (°C) | MAP (mm) | Altitude (m.a.s.l) | Land cover type |
|---|---|---|---|---|---|---|---|---|
| FDE | Fragas do Eume | 43.36926 N, 7.98579 W | Csb | 1.33 | 12.2 | 1361.7 | 450 | Mixed Forests |
| ATK | Artikutza | 43.19830 N, 1.80540 W | Cfb | 1.25 | 12.1 | 1312.6 | 344 | Deciduous Broadleaf Forests |
| LHE | Las Herrerías | 42.66882 N, 6.98307 W | Csb | 1.09 | 11.0 | 1253.3 | 665 | Deciduous Broadleaf Forests |
| ARZ | Arantzazu | 42.96013 N, 2.37830 W | Cfb | 1.00 | 9.4 | 1004.0 | 803 | Deciduous Broadleaf Forests |
| VAL | Vallcebre | 42.20294 N, 1.82094E | Cfb | 0.70 | 9.2 | 859.3 | 1096 | Deciduous Broadleaf Forests |
| GAV | Gavarres | 41.89968 N, 2.91217E | Csa | 0.56 | 13.8 | 719.5 | 259 | Evergreen Needleleaf Forests |
| ALB | Albera | 42.39600 N, 2.98230E | Csa | 0.43 | 14.4 | 590.5 | 154 | Open Shrublands |
| MON | Montgrí | 42.06125 N, 3.12231E | Csa | 0.40 | 14.7 | 550.3 | 103 | Evergreen Needleleaf Forests |
| COY | Coy | 37.94358 N, 1.77985 W | BSk | 0.25 | 13.5 | 401.7 | 925 | Open Shrublands |
| MAL | Malcamino | 37.58771 N, 1.44243 W | BSh | 0.18 | 16.9 | 304.1 | 278 | Grasslands |
| SAN | Santomera | 38.09860 N, 1.03135 W | BWh | 0.18 | 17.1 | 314.2 | 195 | Savannas |
| TAB | Tabernas | 37.00954 N, 2.44254 W | BWk | 0.16 | 17.0 | 265.2 | 283 | Barren |

Subsamples for bacterial biomass were fixed with 2 % formalin and stored at 4 °C until analysis. Soil organic matter composition subsamples were also stored at 4 °C, while subsamples for fungal biomass, nutrients and molecular analyses were frozen at −20 °C. For the physicochemical parameters, samples were dried at 60 °C prior to analysis.

### 2.3. Physicochemical variables

Soil texture was analyzed using the hydrometer method (Gee and Bauder, 1986). Soil water content was determined by measuring the loss in weight after oven-drying fresh soils (105 °C, 48 h). Soil organic matter was measured by combusting the oven-dried soils at 450 °C for 4 h. Water activity was measured with a water activity meter (LabSwift-aw, Novasina AG, Lachen, Switzerland). pH was assessed in a 0.01 M $CaCl_2$ soil solution using a pH meter (2:1 *v/w*) method. Total C and total N were measured in dried (60 °C) fine-grained soils and litter using an elemental analyzer (NC-2500, CE Instruments, Wigan, United Kingdom). Carbon-Nitrogen mass-based ratio (C/N) was calculated with these total C and total N values. Soil total organic C was quantified post HCl-fumigation using an elemental analyzer (Walthert et al., 2010). Soil ammonium and sulfate were extracted from 2.5 g dried-soil with 1 M KCl (KCl:soil 4:1 v/w), followed by filtration through DF 5895–150 ashless paper (Albert LabScience, Dassel, Germany). Ammonium in KCl extracts was determined spectrophotometrically with a FIAS 300 flow injection system (Perkin-Elmer, Waltham, USA). Sulfate was measured with a dx-120 ion chromatography. Available phosphorus (phosphate) was extracted with 0.5 M $NaHCO_3$ ($NaHCO_3$:soil 60:1 v/w) and quantified spectrophotometrically with malachite green using a plate reader (TECAN, Life Sciences, USA) (Kuo, 1996).

### 2.4. Organic matter composition

Water extractable organic matter (WEOM) was extracted and quantified following the method described by Chantigny et al. (2014). Extracts from 30 g of freeze-dried soil with 60 mL of MilliQ were prepared, incubated at 20 °C (dark conditions, 80 rpm agitation, 1 h) and filtered with 0.2 µm nylon filters. Filtered extracts were analyzed through absorbance and fluorescence spectroscopy. UV–visible absorbance spectra were measured on an Agilent 8453 spectrophotometer (Agilent Technologies, Germany). Excitation-Emission matrices (EEMs) were obtained on a fluorescence spectrophotometer (F-7000, Hitachi, Japan). The intensity of the main fluorescence peaks related with dissolved organic matter (DOM) characterization (A, M, C, B, T; Coble, 1996; Parlanti et al., 2000) was obtained from the EEMs. From the

fluorescence and absorbance spectra, several indexes were calculated as indicators for WEOM composition. The Biological Index (BIX) indicates recently produced DOM (Huguet et al., 2009) and the Fluorescence Index (FI) is an indicator of vascular plant-derived (low FI ~1.2) or microbial-derived (high FI ~1.8) origin (Cory and McKnight, 2005). The Humification Index (HIX), an indicator of the degree of DOM humification. The absorbance ratios E2/E3, E3/E4, and E4/E6 are all inversely correlated with aromaticity. The slope ratio ($S_R$), calculated as the ratio between the absorbance slopes at the wavelengths intervals 275–295 and 350–400 nm, is inversely correlated to molecular weight and described to increase upon irradiation (Helms et al., 2008). Further details on the variables and methodological procedure are provided in the Supplementary Material.

### 2.5. DNA extraction and microbial community structure

DNA was isolated from 0.25 g soil samples using the DNeasy Powersoil Pro Kit (Qiagen, Hilden, Germany) and quantified by PicoGreen (Molecular Probes, Eugene, OR, USA) following the manufacturer's instructions (ThermoFisher Scientific, USA). The V3-V4 region of the prokaryotic 16S rRNA gene was amplified by PCR using primers 341F and 801R as described by Frey et al. (2016). Barcoding of amplicons was performed with Fluidigm Access Array technology (Fluidigm) and paired-end sequencing was conducted on the Illumina MiSeq v3 platform (Illumina Inc., San Diego, CA, USA) at the Genome Quebec Innovation Center (Montreal, Canada). Raw sequences were processed using DADA2 (Callahan et al., 2016) in Qiime2 (Bolyen et al., 2019). Primer removal was carried out with cutadapt (Martin, 2011) using default settings, and sequences were quality filtered and denoised with DADA2 (p-trunc-len-f = 270, p-trunc-len-*r* = 220, p-max-ee = 5 for 16S rRNA sequences, p-trunc-len-f = 270, p-trunc-len-*r* = 230, p-max-ee = 4 for ITS sequences). 16S rRNA and ITS2 sequences were classified using the q2-feature-classifier scikit-learn algorithm in Qiime (Bokulich et al., 2018; Pedregosa et al., 2011) with default parameters (p-confidence = 0.7) against the SILVA v138 (Quast et al., 2013) and UNITE v9 (Abarenkov et al., 2010) taxonomic databases, respectively.

### 2.6. Microbial biomass

Prokaryotic density was analyzed by flow cytometry after disaggregation and dilution of the soil prokaryotes. Soil samples were shaken in a disaggregation solution of 2 % formalin and surfactant (150 rpm, 30 min, dark conditions), cooled down and sonicated to separate prokaryotic cells from soil particles. A coagulant agent (Nycodenz Optiprep density gradient, Sigma-Aldrich, Merck KGaA, Darmstadt, Germany) was used to help precipitate particulate material after centrifugation (14,000 rpm, 90 min, 4 °C) and obtain a clean sample. Samples were diluted and stained using a nucleic acid dye (SYTO13, FISHER, 5 μM). Prokaryotic density was measured by flow cytometry (FACSCalibur, Becton Dickinson, Franklin Lakes, USA), using a standard curve of beads at known concentrations. Prokaryotic biomass results were obtained from prokaryotic densities (Bratbak, 1985; Theil-Nielsen and Søndergaard, 1998) and expressed as μg of prokaryotic C per g dry weight (DW) of soil. Fungal biomass was measured through the analysis of ergosterol content in soil samples by high-performance liquid chromatography (HPLC, Waters Corporation, Milford, USA). Ergosterol was extracted from the samples, after soil lyophilization, performing the lipid extraction in alkaline methanol and separating in a solid-liquid phase extraction (Waters Sep-Pak, V ac RC, tC 18, 500 mg) (Gessner, 2005). Considering the stoichiometric relationship from Montgomery et al. (2000), results were expressed as μg of fungal C per g DW of soil.

### 2.7. Microbial aerobic respiration and extracellular enzyme activities

For both microbial aerobic respiration and extracellular enzyme activity (EEA) assays, soil extracts (5 g of fresh soil with 50 mL pH-matched buffer; Maleate buffer for pH 5 to 6, Tris(hydroxymethyl) aminomethane buffer for pH 7 to 8).

Microbial respiration was determined using the resazurin (RAZ) assay. RAZ was added to the sample extracts and to controls (buffer instead of extract), mixed, placed into a black 96-well plate and incubated overnight (dark conditions, at the temperature of the soil during the sampling campaign). Fluorescence measurements were done before and after the incubation with a plate reader (Infinite M200 Pro, Tecan, Zurich, Switzerland) at 602/632 nm excitation/emission wavelengths. RAZ results were obtained through the difference between the final and initial fluorescence. To convert fluorescence to RAZ concentration, a calibration curve was used (0–100 μg/L). Results were expressed as pmol of RAZ transformed per g DW per hour of incubation.

Eight EEA related to the degradation of different labile to recalcitrant C and N compounds were analyzed: α-glucosidase (ALPHA); β-glucosidase (BETA); β-xylosidase (XYL); cellobiohydrolase (CBH); *N*-acetyl-β-glucosaminidase (NAG); phosphatase (PHOS); leucine-aminopeptidase (LEU); and phenol oxidase (PHE). Soil extracts were incubated with artificial substrates under saturation (Table S2) at field temperature conditions. For the hydrolytic enzymes (all except PHE), incubations lasted one hour, and after them, glycine buffer (0.05 M, pH 10.4, mixed at a 1:1 ratio v:v) was added to all samples, standards (ranging from 0 to 100 μM for MUF: methylumbelliferone, and AMC: 7-Amino-4-methylcoumarin), controls (samples without artificial substrate) and quenching controls (samples plus a MUF/AMC standard). Fluorescence was measured with a microplate reader (Infinite M200 Pro, Tecan, Zurich, Switzerland) at 365/455 nm for MUF and 364/445 nm for AMC excitation/emission wavelengths. Final results were quantified as the rate of MUF or AMC released per hour relative to the soil dry weight (μmol MUF or AMC * g $DW^{-1}$ * $hour^{-1}$). PHE activity was assessed by spectrophotometry using L-DOPA (3,4-Dihydroxy-*L*-phenylalanine) as a substrate (Table S2). Samples, controls (L-DOPA with buffer) and blanks (soil extract with buffer) were incubated for 2 h in the dark. Additionally, the absorbance from the buffer alone was measured separately. Absorbance measurements were read at 460 nm (Infinite M200 Pro, Tecan, Zurich, Switzerland). The results were expressed as μmol of DIQC (3-dihydroindole-5,6-quinone-2-carboxylate; the product of the L-DOPA reaction) per hour relative to the dry weight of the soil (μmol of DIQC * g $DW^{-1}$ * $hour^{-1}$).

With the data from the eight different enzyme activities, a multifunctionality index has been calculated in the form of a Shannon diversity index. Enzyme activities were first standardized to consider differences in measurement and units. The relative contribution of each enzyme to the total enzyme activity ($p_i$) was calculated per sample and used to compute the Shannon index using the formula $-\sum(p_i * \log_2 p_i)$.

### 2.8. Data analyses

Different matrices of variables have been used for analyzing the data. The climatic variable matrix includes the variables extracted from the worldclim database (AI, MAT and MAP), as well as altitude. Regarding soil characteristics, this matrix includes the physicochemical variables (soil temperature, water content, water activity, soil organic matter, pH, total C, total N, total organic C, C/N, Litter, LTC, LTN, ammonium, sulfate, phosphorous), soil texture (Sand, Silt and Clay content) and the organic matter quality indexes (S275–295, S350–400, $S_R$, E2/E3, E3/E4, E4/E6, FI, BIX, HIX and Peaks A, B, C, M, T). An environmental matrix which includes the climatic and soil characteristics variables together has been used to perform some analyses. Microbial community composition matrices are related to the prokaryotes or fungi sequencing (Amplicon Sequence Variants, ASVs). The functional matrix includes the extracellular enzyme activities (ALPHA, BETA, XYL, CBH, NAG, PHOS, LEU, PHE) and the aerobic microbial respiration. All statistical analyses and plots were conducted in R, version 4.1.2 (R Core Team, 2021).

Alpha-diversity parameters (Chao and Shannon indices) were calculated after rarefying to even sequencing depth, resulting in a total

of 356,040 and 113,880 sequences for 16S rRNA gene and fungal ITS2 region respectively. Differences in composition among the microbial communities between sites were tested through permutational multivariate analysis of variance (PERMANOVA, permutations = 10,000) with the "*adonis2*" function, from the *vegan* package (Oksanen et al., 2022), based on Bray-Curtis distances of relative abundances. These results were graphically represented with Principal Coordinates Analysis (PCoA).

For the soil functions and microbial biomass, linear mixed effects models with site as a random factor, were used to decipher the most relevant driving variables, including soil characteristics and climate variables. Collinearity among variables was assessed using the "*vif*" function from the *usdm* package (Naimi et al., 2014), setting a threshold of 10 for the VIF values. The selected variables were soil temperature, soil organic matter, pH, C/N, ammonium, phosphate, sulfate, Silt, Litter, LTC, LTN, LTC/LTN, prokaryote biomass (PB), $S_R$, E2/E3, E4/E6, BIX, Peak C, Peak B, HIX, and altitude. To further refine the models, additional variables which were deemed potentially significant were incorporated using the "*vifstep*" function, including water content, total C, fungal biomass (FB), and Clay. Although aridity was correlated with other variables, it was also added to the models in order to test its potential effects on the soil functions. The linear mixed effect models were constructed using the "*lmer*" functions from the *lme4* package (Bates et al., 2015). Model diagnostics were performed by examining residuals to check for normality and homoscedasticity. A stepwise model simplification to retain only the most significant predictors was done with the *buildmer* package (Voeten, 2023). Best fits of the models were determined using AIC and $R^2$, through the package *MuMIn* (Barton, 2022). Standardized dominance of each main predicting variable was determined through the function "*domin*" from the *domir* package (Luchman, 2024).

To test for relationships between the soil functions, the microbial community structure, the soil characteristics, the land cover type, and the climatic variables (AI, MAT, MAP, and altitude), Mantel tests (method = Spearman, permutations = 100,000) were conducted with the distance matrices derived from each variable group. Land cover, originally a categorical variable, was transformed into a binary dummy matrix of each land cover type per site, and Jaccard distance was used to calculate pairwise dissimilarities. All numerical variables were standardized and transformed into Euclidean distance matrices before performing the Mantel tests. For both the Mantel tests and the linear mixed models, some correlated and conceptually similar variables were aggregated, and thus the enzymes involved in the degradation of simple polysaccharides (ALPHA and BETA), and the enzymes involved in the degradation of hemicellulose and cellulose (XYL and CBH) were aggregated. Additionally, for the linear mixed models, the microbial biomass (PB and FB) was aggregated as a unique variable (microbial biomass, MB).

Further data analysis that complements the primary findings are included in the Supplementary Material.

## 3. Results

### 3.1. Climatic and physicochemical description

As expected, soil water content correlated negatively with aridity (Table S3). pH and C/N ranged from 3.78 ± 0.1 to 7.71 and from 12.2 ± 0.6 to 90.0 ± 18.7 respectively (Table S1), and both had a significant positive correlation with aridity (Table S3). Conversely, LTN, LTC and phosphates were negatively correlated with aridity (Table S3). Soil texture did not follow a clear trend with aridity (Fig. S2, Table S3). Sampling sites were separated according to their aridity in a PCA based on all soil physicochemical variables, with PC1 and PC2 explaining a 50.0 % of the total variation observed (Fig. S3). As expected from the correlation analyses (Table S3), most arid sites were characterized by high soil pH and C/N, while most humid sites were characterized by high C and N litter content, and high soil phosphate content. Among humid sites, further variability in soil characteristics was found, and ATK and FDE showed high silt content and BIX (Table S4), while VAL showed high ammonium and total C content (Table S1).

### 3.2. Microbial community diversity and composition along the aridity gradient

The total number of Amplicon Sequence Variants (ASVs) for prokaryotes and fungi were 4932 (with 577,639 total reads) and 4536 (768,004 total reads), respectively. When analyzing prokaryotic community α-diversity, we found no correlations between aridity and the observed number of ASVs (Richness) or the Shannon and Chao indices for 16S rRNA gene fragments (Table S3, Table S5). In contrast, fungal community Shannon and Chao indices were negatively correlated with aridity (Table S3). The prokaryotic and fungal community structures differed between sites and clustered according to aridity (PERMANOVA ~ Site, F = 6.21, *p*-value <0.01 for prokaryotes, Fig. 2A; PERMANOVA ~ Site, F = 3.97, p-value <0.01 for fungi, Fig. 2B; Fig. S4).

Across all samples, the most abundant prokaryotic phyla were Planctomycetota (average of 24.6 % across all samples), Pseudomonadota (20.7 %) and Verrucomicrobiota (15.9 %), followed by Actinomycetota (12.8 %) and Chloroflexota (10.4 %). Chloroflexota and Actinomycetota relative abundances increased with aridity; in the less arid site (FDE), their relative abundances were 3.9 % and 8.0 %, respectively, and increased to 33.1 % and 24.2 % at the most arid site (TAB) (Fig. 3A). In contrast, other phyla relative abundances decreased with aridity; Pseudomonadota ranged from 31.3 % in FDE to around 11 % in the most arid sites (MAL and TAB), Verrucomicrobiota were the lowest at the four most arid sites, and Acidobacteriota gradually decreased from semi-arid (around 11 %) to arid sites (from 3 % to 7 %) (Fig. 3A).

For fungi, the most abundant classes across all samples were Agaricomycetes (average of 21.5 % across all samples), Eurotiomycetes (18.9 %) and Dothideomycetes (10.9 %), followed by Leotiomycetes (9.9 %), Sordariomycetes (9.5 %) and Pezizomycetes (6.9 %) (Fig. 3B). Dothideomycetes and Eurotiomycetes classes increased with aridity (ranging from values of 1–5 % and 4–9 % in the less arid sites to 25.5 % and 35.6 % relative abundance in the most arid site), while Agaricomycetes decreased with aridity (25–36 % to 2.1 %) (Fig. 3B).

Both the prokaryotic and fungal community matrices were strongly correlated with the climatic matrix, showing weaker but also significant correlation to soil characteristics (Mantel tests, Table 2). Specifically, most influencing environmental variables were aridity, MAP and pH (Fig. S5, Table S6).

### 3.3. Microbial biomass and soil functions along the aridity gradient

Prokaryotic biomass ranged from 0.73 ± 0.24 to 8.77 ± 2.20 μg C $g^{-1}$ DW, and fungal biomass from 144.94 ± 56.41 to 1700.29 ± 208.81 μg C $g^{-1}$ DW. These ranges do not include a site within the gradient (VAL), which had unexpectedly high prokaryotic (17.78 ± 2.92 μg C $g^{-1}$ DW) and fungal (8530.12 ± 1696.09 μg C $g^{-1}$ DW) biomass (Fig. S6). Neither prokaryotic nor fungal biomass had a significant correlation with aridity, regardless of whether VAL was included or not (Fig. S6). Microbial biomass was mainly driven by total soil C content (positively) and peak B -indicator of protein compounds in WEOM- (negatively) and, although not statistically significant, by water content and clay content (Fig. 4).

Microbial aerobic respiration ranged from 28.10 ± 2.09 to 71.12 ± 2.28 pmol Raz $g^{-1}$ DW x $h^{-1}$ and was not correlated with aridity (Fig. S7, Table S3). Microbial respiration was mainly driven by clay content interacting with aridity (Fig. S8), and to a lesser extent by water content and the BIX index (Fig. 4).

Among all enzymes measured, ALPHA was the only that correlated positively with aridity (Fig. S9, Table S3). The functional matrix showed

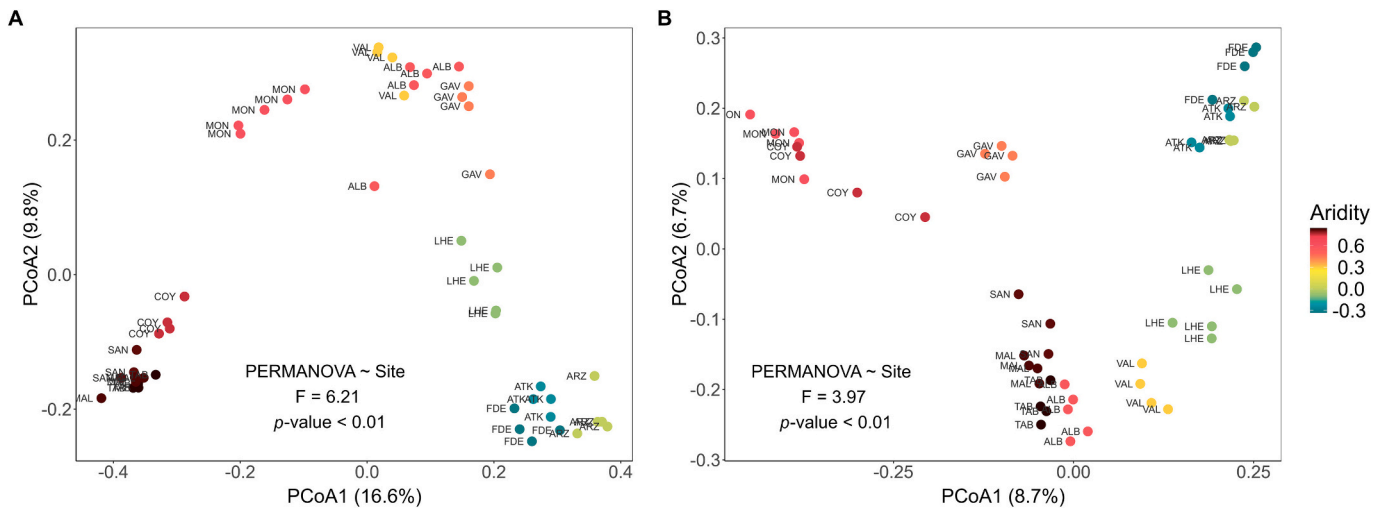


**Fig. 2.** Principal Coordinates Analyses (PCoA) for the total of ASVs observed for prokaryotic (A) and fungal (B) communities. Each dot represents a replicate soil sample from each site; dots are colored according to the aridity gradient scale (Aridity = 1 - Aridity Index). Letters next to the dots represent the site codes. PERMANOVA test results to assess differences in the microbial community structure between sites are shown in each respective plot. Bray-Curtis distances were used based on taxa relative abundance.

a significant correlation to soil characteristics, followed by prokaryote community and climatic variables matrices, in order of strength ($R^2$, Mantel test, Table 2). Functions did not follow a clear aridity gradient (Fig. S10), nor did the soil multifunctionality index (Fig. S11). Instead, their variability was mainly explained by soil C content (total C, total organic C) and quality (HIX), litter content (LTC, LTN), texture (silt), pH, and two variables related to climate (water content and soil temperature) (Fig. S12). In more detail, each specific EEA showed different drivers (Fig. 5). Enzymes related to the degradation of litter compounds, like hemicellulose and cellulose (XYL and CBH), were driven by total C and silt content interacting with aridity (Fig. S8). In contrast, enzymes involved in the degradation of simple polysaccharides (ALPHA and BETA) were primarily driven by soil temperature. The degree of humification of the organic matter (HIX) influenced all these enzymes, either interacting with aridity (Fig. S8) or not. Organic matter availability (soil organic matter and total C) mainly drove the enzymes related to lignin degradation (PHE) and to nutrient acquisition (PHOS, LEU, and NAG to a lesser extent). Finally, water content contributed significantly to NAG activity and microbial respiration, but not on the other functions. The results for each model, with the statistics for each main driver separately, are shown in the supplementary data (Table S7).

Structural equation modeling (SEM) for all enzymes aggregated (Fig. S13), or for each function separately (Fig. S14), showed an overall acceptable to good model fit (Table S8), and pointed that aridity affected functions indirectly (Table S9), thought its influence on soil properties, and in most cases, in microbial community composition. Aridity consistently reduced prokaryotic composition ($r = -0.89$, $p$-value $<0.001$), and strongly influenced soil properties, while these variables affected each specific function.

## 4. Discussion

### 4.1. Aridity shapes soil microbial community structure

The prokaryotic and fungal community structure clearly changes within the studied aridity gradient, ranging from humid to semi-arid and arid soils (AI from 1.25 to 0.18). Other studies have shown shifts in microbial community structure along aridity gradients, with reductions in the abundance and diversity of the microbial community as aridity increases (Maestre et al., 2015; Neilson et al., 2017; X. Wang et al., 2024). However, these studies included narrower aridity ranges, such as considering only drylands or forests, whereas our study covers a wide aridity range (i.e., from humid to arid) which allows deciphering more representative patterns.

Increasing aridity determined the reduction of Pseudomonadota, Verrucomicrobiota and Acidobacteriota prokaryote phyla. The effect of aridity on Pseudomonadota from previous studies is unclear, as some show a negative relationship (Li et al., 2022; Neilson et al., 2012), and others a positive one, especially when studying only drylands and up to hyper-arid soils (Dong et al., 2024; Maestre et al., 2015; McHugh et al., 2017). Although we observed a clear tendency for Pseudomonadota to decrease with aridity (up to arid soils), its metabolic versatility could make species of this phylum resistant to highly desiccated environments, such as in hyper-arid soils (Leung et al., 2020). The decrease in Verrucomicrobiota in arid soils is expected, as this phylum has affinity to humid soils (N. Liu et al., 2023). Acidobacteriota showed a gradual decrease only from semi-arid to arid soils, which may be related to its affinity for soils with low pH, more common in humid climates (Conradie and Jacobs, 2021), and have shown positively correlation with MAP and negative with MAT and aridity (Dong et al., 2024).

The fungal community structure was also clearly affected by aridity, as it showed a decrease in the Agaricomycetes and Leotiomycetes classes' relative abundances. These changes might be related to the decrease in vegetation cover and litter with aridity. Given that fungi serve as the primary decomposers of lignin, cellulose and hemicellulose, fluctuations in woody material may influence the fungal community structure along the aridity gradient (Abrahão et al., 2019). Specifically, Agaricomycetes, as wood-decay fungi, are shown to be affected by the quality and quantity of woody substrates (Eduardo et al., 2018). This decrease in Agaricomycetes correlated with lower levels of litter mass and was evident in the sampled sites with less woody vegetation, such as the two most arid sites along the gradient, which had grassland and barren as land cover types. Apart from wood rot fungi, Leotiomycetes class is ecologically diverse, including mycorrhizae and root symbionts (Ekanayaka et al., 2019; Johnston et al., 2019), and therefore related to plant roots development and similarly affected by decreasing higher plant development.

Conversely, certain prokaryotic (Chloroflexota and Actinomycetota phyla) and fungal (Dothideomycetes and Eurotiomycetes classes) groups became more abundant in their respective communities as aridity increased. These phyla are known to be well adapted to dryland environments (Cowan et al., 2022; Makhalanyane et al., 2015). Both Chloroflexota and Actinomycetota are Gram-positive bacteria, which imply thick cell walls that help them withstand arid conditions.

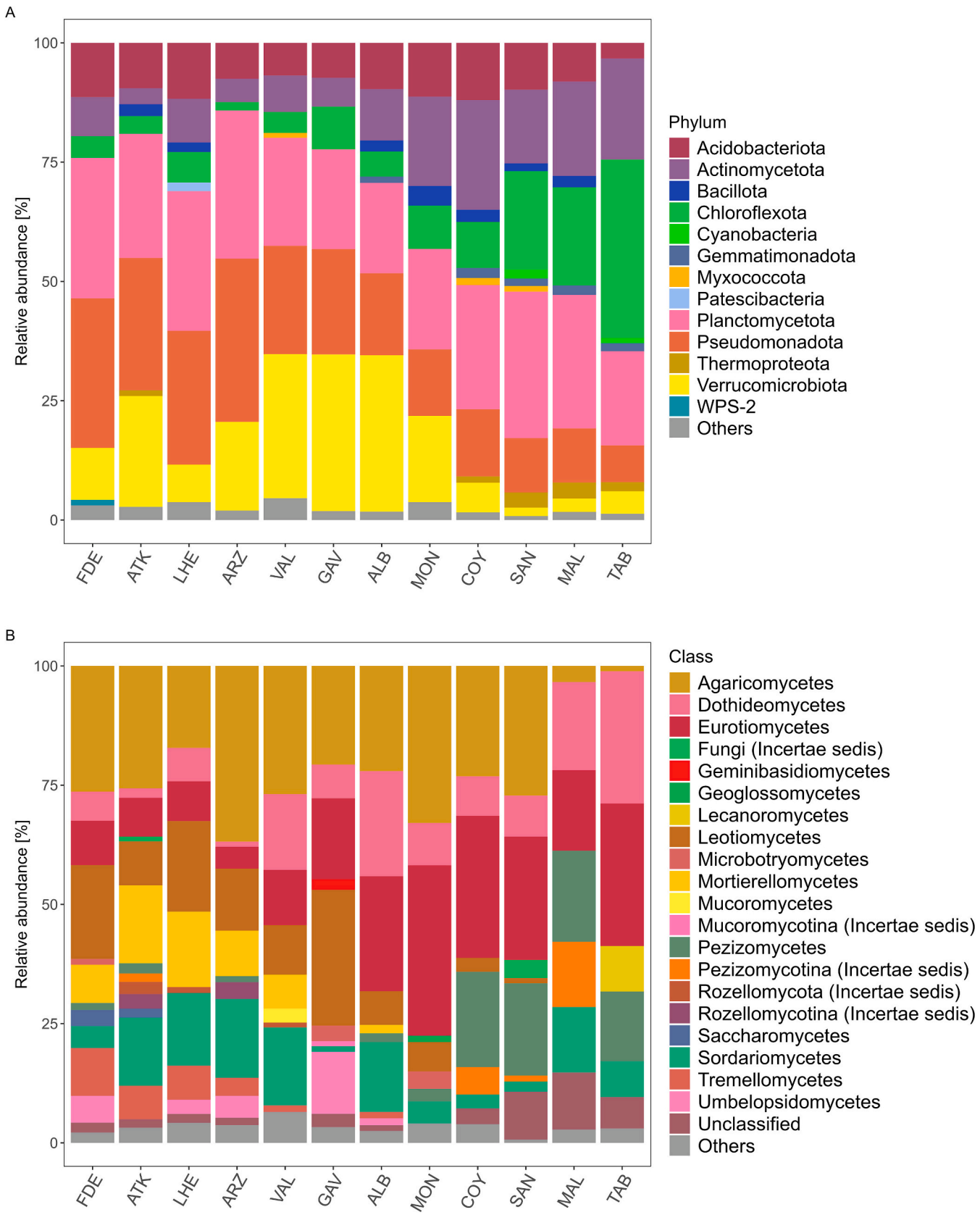


**Fig. 3.** Relative abundances of the main prokaryotic phylum (A) and fungal classes (B) in each sampling site. Sites are ordered left to right from the least to the most arid. "Others" refers to phyla or classes representing <1% of the sequences in the respective site.

**Table 2**
Mantel test results for the different variable datasets. AI = Aridity Index. MAT = Mean Annual Temperature (°C). MAP = Mean Annual Precipitation (mm). n.s. = non-significant.

| | Soil characteristics | Functional variables | Microbial community composition | | Land cover type |
|---|---|---|---|---|---|
| | | | Prokaryotes | Fungi | |
| Soil characteristics | – | $R^2 = 0.44$<br>p-value = 0.02 | $R^2 = 0.40$<br>p-value <0.01 | $R^2 = 0.34$<br>*p*-value <0.01 | $R^2 = 0.07$<br>p-value = n.s. |
| Climatic variables (AI, MAT, MAP, altitude) | $R^2 = 0.55$<br>p-value <0.01 | $R^2 = 0.23$<br>p-value = 0.02 | $R^2 = 0.63$<br>p-value <0.01 | $R^2 = 0.65$<br>p-value <0.01 | $R^2 = 0.34$<br>p-value = 0.02 |
| Functional variables | $R^2 = 0.44$<br>p-value = 0.02 | – | $R^2 = 0.27$<br>p-value = 0.02 | $R^2 = 0.14$<br>p-value = n.s. | $R^2 = -0.04$<br>p-value = n.s. |

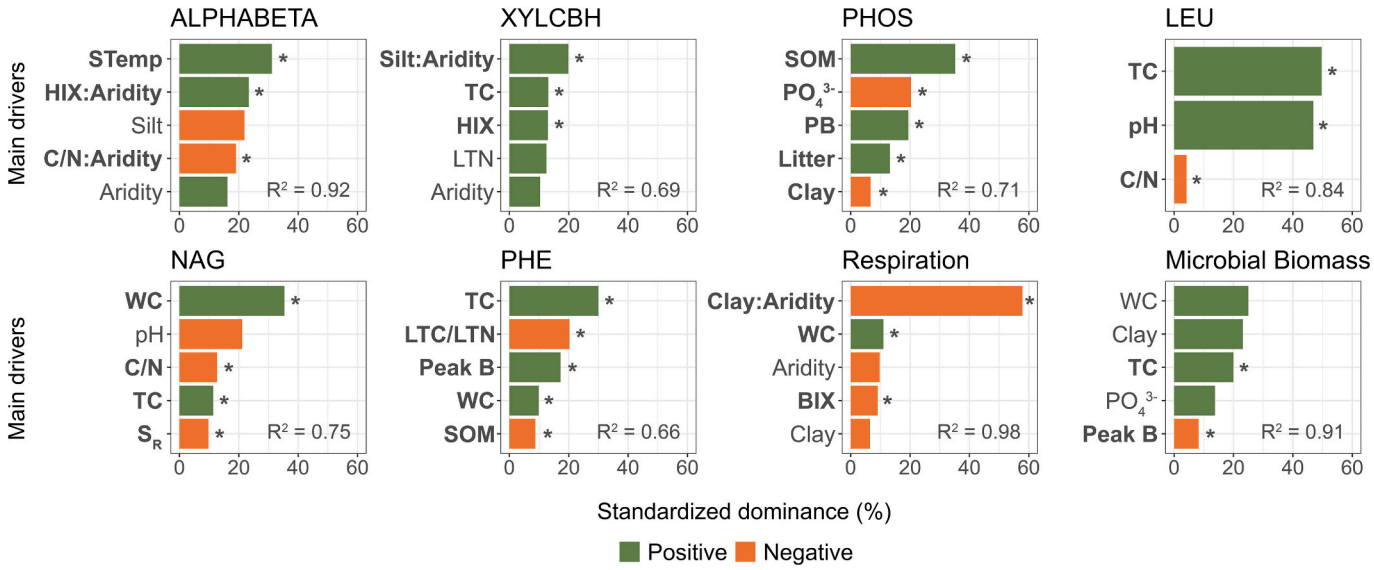


**Fig. 4.** Standardized dominance (%) of the main predicting variables for each model. In bold and with asterisks are shown the significant predictors for each model (p-value < 0.05). Conditional R squared is shown for each model. ALPHABETA = ALPHA + BETA activities; XYLCBH = XYL + CBH activities; PHOS = phosphatase; LEU = leu-aminopeptidase; NAG = N-acetyl-β-glucosaminidase; PHE = phenol oxidase. Microbial Biomass includes PB (Prokaryotic Biomass) and FB (Fungal Biomass). BIX = biological index; HIX = humification index; LTC = total carbon in the litter; LTN = total nitrogen in the litter; PeakB = indicator of protein compounds in WEOM; $PO_4^{3-}$ = phosphate concentration; SOM = Soil organic matter; STemp = Soil Temperature; $S_R$ = Slope Ratio; TC = total carbon; WC = water content.

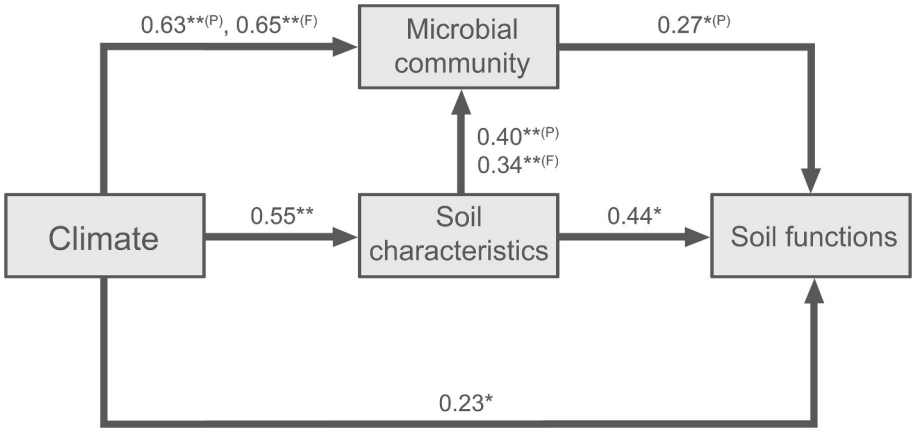


**Fig. 5.** Conceptual framework showing the effects of climate (aridity, mean annual temperature [MAT], mean annual precipitation [MAP], and altitude) on the studied soil functions through soil characteristics and microbial community. Path coefficients represent significant correlations after Mantel tests (see Table 2). Asterisks indicate significance levels (*$p$-value < 0.05, **$p$-value < 0.01). Superscripts indicate the microbial group involved: (P) for prokaryotes, and (F) for fungi. Further details on direct and indirect pathways are shown in the structural equation models (Fig. S13 and S14; Table S9).

Moreover, their capacity to form endospores and synthesize osmolytes further enhances their resistance to aridity (Marasco et al., 2021). Therefore, observing the highest proportion of Actinomycetota with aridity was expected (Dong et al., 2024; Leung et al., 2020; Makhalanyane et al., 2015; Neilson et al., 2017). Chloroflexota are primary producers and common components of biological soil crusts (BSC)

(Mugnai et al., 2024). Therefore, it was also unsurprising to observe the highest abundance of this phylum specially in the most arid and BSC-covered site of the gradient ("Desierto de Tabernas") (Lázaro et al., 2022; Maestre et al., 2015; Maier et al., 2018). Although Cyanobacteria do not show an increasing pattern with aridity, they were only detected at low relative abundance in some of the most arid sites. This could be attributed to their prevalence in BSC, as it has been indicated that while Cyanobacteria are abundant in BSC, they are not as common once vegetation cover increases with decreasing aridity (Guo et al., 2023; Leung et al., 2020). Regarding fungi, Dothideomycetes and Eurotiomycetes are black yeast fungi, which are renowned for their capacity to resist UV radiation (Coleine et al., 2022). Due to this characteristic, their presence within the community in high aridity soils is crucial, as they form an opaque barrier over photobionts, shielding them against harmful UV radiation (Dong et al., 2024).

Our results indicate that climate (i.e. MAT, MAP and AI) strongly shapes the soil prokaryotic and fungal community structure whereas soil characteristics play a weaker role. Despite these compositional shifts, microbial biomass did not vary with aridity, suggesting that community adaptation likely occurred through taxonomic reorganization, buffering potential changes in biomass (Yang et al., 2022). Interestingly, the hierarchical clustering of sites along the aridity gradient differed between prokaryotes and fungi, being the latter more erratic, with sites often grouped together despite having quite different aridity levels. This suggests that prokaryotes and fungi do not respond in the same way to differences in aridity. Similar to the results from S. Wang et al. (2021), soil prokaryotes seem to adapt through aridity shifts changing their taxa proportions, whereas fungi display greater variability across sites, with only few fungal classes consistently present across all environments. Reduction of fungal classes as aridity increases must be related to the reduction of fungal diversity found in this study. The lack of consistent dominant taxa suggests that increasing aridity filters fungal groups that are less tolerant to water stress, leading to community simplification, and consequently, a decrease in diversity. Moreover, most fungi are commonly more strongly coupled to plant community development than bacteria (X. Wang et al., 2024) and therefore being more sensitive to reduction in vegetation cover shaped by aridity.

### 4.2. *Indirect effects of aridity on soil functions via changes in microbial community*

In contrast to our hypothesis, soil functions did not clearly decrease with aridity. This suggests that, whereas the microbial community structure at each site reflects its long-term adaptation to climate, soil functions are more related to the local edaphic environment. Still, indirect effects of aridity on soil functions through changes in community structure -mainly prokaryotes- may occur (Fig. 5).

This might be specially the case for those enzyme activities that seem to follow better the aridity gradient and/or that are related to the community structure (i.e. α- and β-glucosidases and cellobiohydrolase). For example, Actinomycetota and Chloroflexota phyla, which increase under arid conditions, both carry genes capable of producing glycoside hydrolases, such as α- and β-glucosidades (Zang et al., 2017; Zhang et al., 2024). Also, Eurotiomycetes, which are xerotolerant fungi, have a positive relationship with α- and β-glucosidase, β-xylosidase, and cellobiohydrolase activities (J. Wang et al., 2020). Likewise, Pseudomonadota and Acidobacteriota, both predominant phyla in more humid sites, exhibit high phosphatase activity (Azene et al., 2023). Pseudomonadota also possess a wide range of enzymes for degrading C compounds, including *N*-acetyl-β-glucosaminidase, and Acidobacteriota demonstrates an enhanced capacity for *N*-acetyl-β-glucosaminidase production (Lladó et al., 2016). Accordingly, these enzyme traits could be related to the higher production of phosphatase and *N*-acetyl-β-glucosaminidase in the humid sites of this study.

In addition, the weak relationship between aridity and soil functions in parallel to the clear aridity-shaped community composition, may also indicate microbial functional redundancy. In soils, functional redundancy is commonly observed, particularly in more arid environments compared to moister ones (León-Sobrino et al., 2019; Song et al., 2019). This common characteristic of functional redundancy in soils may arise from the non-monophyletic nature of many functions, meaning that certain functions are not exclusive to a single phylogenetic group (Louca et al., 2018). The fact that prokaryotes had a (weak) correlation with soil functions, while fungi had not, could be related to a greater functional redundancy of fungi than bacteria (Starke et al., 2020).

### 4.3. *Mainly soil characteristics, sometimes interacting with aridity, drive soil functioning*

In this study, soil microbial functions have shown to be primarily driven by variables related to soil texture, organic matter quantity and quality, and pH, rather than by climatic variables. Aridity was not the main driver of any soil function individually, but other climate-related variables (such as water content and soil temperature), and factors interacting with aridity, appeared as relevant drivers. Accordingly, along the studied aridity gradient, climate is shown to play an indirect role in soil functions. However, it must be considered that aridity, MAT and MAP climate values, were obtained from a database with 1 × 1 km resolution and averaged over 30 years. This may imply that, although the long-term data allow a climatic gradient classification, there is a limitation in capturing the exact conditions at each site during the year of the sampling. This limitation could hinder the potential link between aridity and/or other climate variables and soil respiration and organic matter enzyme degradation potential.

Interestingly, the different soil functions studied have shown distinct drivers. Soil texture (silt and/or clay) interacting with aridity, appears as a significant factor for enzymes involved in cellulose (cellobiohydrolase) and hemicellulose degradation (β-xylosidase) and soil respiration. The relationship between soil texture and the organic matter content and the availability of C substrates has been long reported, showing, in general, positive effects of silt and clay percentages on soil C content and water-holding capacity (Augustin and Cihacek, 2016; Hassink, 1997). However, here we found a negative effect of silt content on β-xylosidase and cellobiohydrolase activities at the most humid sites, but a positive effect at the most arid ones. This suggests that in the highly arid soils, silt may favor litter (substrate for β-xylosidase and cellobiohydrolase) and water retention for their microbial degradation, as these soils are characterized by low litter and water content. In contrast, in humid soils, increasing silt content may favor the formation of silt-organic matter-enzyme colloids limiting enzyme diffusion and activity (Guber et al., 2022).

Soil respiration also showed an interactive effect with aridity and texture (clay content), but in this case, the increase in percentage of clay determined low respiration in the more arid soils. Clay content may have contrasting effects; while clay enhances organic matter retention, favoring microbial colonization, it can also reduce the bioavailability of organic matter to microorganisms (Rakhsh et al., 2020). Our results suggest a general positive effect of clay content on microbial biomass but, at the more arid and higher clay content sites, organic matter mobilization may be reduced with negative consequences for respiration.

As expected, most enzyme activities (β-xylosidase and cellobiohydrolase, phenol oxidase, *N*-acetyl-β-glucosaminidase, phosphatase, leucine-aminopeptidase), as well as microbial biomass, showed a positive effect of organic matter quantity (i.e., total C, soil organic matter, litter content) as indicators of the resource availability for microbial degradation (Stock et al., 2019). However, most functions were also affected by organic matter quality (WEOM indexes, and C/N ratios from soil and litter), which might more specifically reflect organic matter bioavailability. Specifically, the degree of humification (HIX) positively affects β-xylosidase and cellobiohydrolase activities, and also degradation of starch and simple polysaccharides (α- and β-glucosidase activities), at high aridity levels. Although HIX is not correlated to aridity, it

tends to decrease at more arid sites, probably being related to the vegetation type (i.e., the reduced cover of woody and tree vegetation, which is a primary source of aromatic compounds). The increase in HIX may indicate a higher availability of mainly C organic substrates, and thus enhancing simple and complex degradation of polysaccharides. This effect could be more relevant in arid sites where organic matter inputs from vegetation are scarce.

Similarly to the C-degrading enzymes, lignin degradation activity (phenol oxidase) was enhanced by organic matter quality variables, like the protein-like compounds in WEOM (peak B), together with low C/N in litter. Probably, some plant derived proteins (contributing to peak B) contain bonds with phenolic compounds, which phenol oxidase can break down (Matheis and Whitaker, 1984). Also, low C/N ratios may contribute to enhancing decomposition of recalcitrant lignified compounds (Theuerl et al., 2010). Aridity was not a main driver for phenol oxidase, however, this enzyme was affected by water content, showing a general tendency to be higher in humid sites. However, as further described by other authors, phenol oxidase appears to be more influenced by the soil organic matter content than by climatic factors (Tan et al., 2021).

Chitin degradation (*N*-acetyl-β-glucosaminidase activity) is a key enzyme that provides not only C but also N to microbes. It was also affected by C quantity and quality, but its main driver was soil water content. Humid soils may enhance the development of organisms containing chitin such as microfauna and fungi (Bärlocher and Porter, 1986; Brown et al., 2019), increasing the availability of the substrate for this enzyme (Gionchetta et al., 2019; Kwok et al., 2016; Morón-Ríos et al., 2010).

The nutrient-acquiring enzymes (phosphatase, leucine-aminopeptidase) did not show any direct relationship with aridity or any climatic factor, suggesting that these are mostly driven by substrate availability. Phosphatase, in particular, is strongly correlated with organic matter components in other studies (Salazar et al., 2011), likely due to the influence of soil organic matter to phosphatase through the creation of stable humus-enzyme complexes (Nannipieri et al., 1988). For leucine-aminopeptidase, soil pH may be key for substrate availability, as soil surface N mineralization at local or regional scales has been found to be positively related with soil pH (Y. Liu et al., 2016). Although leucine-aminopeptidase has an optimal pH of 7.2 (Balume et al., 2022), unlike other enzymes, it can maintain high activity at higher pH values (Puissant et al., 2019).

## 5. Conclusions

In the soils from the studied aridity gradient, climate strongly shapes the microbial community, while soil functions are mainly determined by physical and chemical characteristics of the soil. However, climate exerts a significant indirect effect on the soil functions through the prokaryotic community and by modifying key soil characteristics, such as water content and organic matter quality. This indicates soil functions being part of the soil ensemble of long-term adapted natural environments, functioning as a laced gear. But this further suggests that if not all actors of the ensemble (i.e. soil characteristics, microbial community, vegetation cover) respond in a similar velocity to climate change conditions such as dryness, soil functions and in consequence global cycles may be compromised. This study highlights the complexity of the regulation of soil system functionality, and consequently, points that policies aimed at mitigating the effects of climate change should be site-specific, taking into account the particular physical and chemical properties of each soil.

## CRediT authorship contribution statement

**Anna Doménech-Pascual:** Writing – original draft, Formal analysis, Methodology, Visualization, Writing – review & editing, Conceptualization. **Luciana Chavez Rodriguez:** Writing – review & editing, Formal analysis, Supervision, Visualization. **Xingguo Han:** Data curation, Writing – review & editing, Conceptualization. **Joan Pere Casas-Ruiz:** Methodology, Writing – review & editing, Conceptualization, Supervision. **Joan Ferriol-Ciurana:** Writing – review & editing, Data curation, Methodology. **Jonathan Donhauser:** Data curation, Writing – review & editing, Conceptualization. **Karen Jordaan:** Conceptualization. **Steven D. Allison:** Supervision, Writing – review & editing. **Aline Frossard:** Writing – review & editing, Conceptualization, Funding acquisition, Project administration. **Anders Priemé:** Funding acquisition, Project administration, Writing – review & editing, Conceptualization. **Jean-Baptiste Ramond:** Conceptualization, Project administration, Writing – review & editing, Funding acquisition. **Anna M. Romaní:** Funding acquisition, Supervision, Writing – original draft, Writing – review & editing, Conceptualization, Project administration.

## Declaration of competing interest

The authors declare the following financial interests/personal relationships which may be considered as potential competing interests:

Anna Doménech-Pascual reports financial support was provided by Government of Catalonia Agency for Administration of University and Research Grants. Anna Maria Romaní Cornet reports was provided by State Agency of Research. Aline Frossard reports was provided by Swiss National Science Foundation. Anders Priemé reports was provided by Innovation Fund Denmark. Jean-Baptiste Ramond reports was provided by South Africa Department of Science and Innovation. If there are other authors, they declare that they have no known competing financial interests or personal relationships that could have appeared to influence the work reported in this paper.

## Acknowledgements

Financial support was provided by the Spanish State Research Agency (PCI2020-120702-2/ AEI/10.13039/501100011033), the Swiss National Science Foundation (SNF 31BD30_193667), the Innovation Fund Denmark (BiodivClim-76 GRADCATCH), and the Department of Science and Innovation of the Republic of South Africa through the 2019-2020 BiodivERsA joint call for research proposals, under the BiodivClim ERA-Net COFUND programme; and partially supported by the Agency for Management of University and Research Grants from the Government of Catalunya (Grant Number: 2021 FISDU 00297). AMR acknowledges the funding from the AGAUR-ICREA Academia award (Catalan Institution for Research and Advanced Studies, ref. 2024 ICREA 00144). We acknowledge the Aizkorri-Aratz parke naturala, Artikutza parke naturala, Consorci de les Gavarres, Parc Natural del Montgrí, les Illes Medes i el Baix Ter, Finca experimental from Centro de Edafología y Biología Aplicada del Segura (CEBAS-CSIC), and the Estación Experimental de Zonas Áridas (EEZA-CSIC) for the access to the field sites. We also thank Gonzalo González Barberá, Carlos Franco, Fermin Lezeta, Consuelo Rubio Gómez-Roso, Oriol Granyer, Pilar Llorens, Roberto Lázaro Suau, Iñaki Uranga, and Xavier Ormazabal for their help in designing and conducting the sampling campaign performed in this study. ADP also acknowledges Alberto Barrón-Sandoval at the University of California Irvine, for his support during the bioinformatics analysis of the DNA sequencing data.

## Appendix A. Supplementary data

Supplementary data to this article can be found online at https://doi.org/10.1016/j.apsoil.2025.106313.

## Data availability

Sequences for 16S rRNA gene fragments and fungal ITS2 region were submitted to the NCBI Sequence Read Archive under the accession numbers PRJNA1073882 and PRJNA1161578, respectively. Data and

code related to the modeling available in the repository: https://github.com/AnnaDomePas/SP_gradient. All other data are available from the authors on request.

## References


Abarenkov, K., Nilsson, R.H., Larsson, K.-H., Alexander, I.J., Eberhardt, U., Erland, S., Høiland, K., Kjøller, R., Larsson, E., Pennanen, T., Sen, R., Taylor, A.F.S., Tedersoo, L., Ursing, B.M., Vrålstad, T., Liimatainen, K., Peintner, U., Kõljalg, U., 2010. The UNITE database for molecular identification of fungi – recent updates and future perspectives. New Phytol. 186 (2), 281–285.

Abrahão, M., Pires, R.M., Gugliotta, A.D.M., Gomes, E.P.C., Bononi, V.L.R., 2019. Wood-decay fungi (Agaricomycetes, Basidiomycota) in three physiognomies in the Savannah region in Brazil. Hoehnea 46 (1), e692018. https://doi.org/10.1590/2236-8906-69/2018.

AppEEARS Team, 2024. Application for extracting and exploring analysis ready samples (AppEEARS), version 3.63 [computer software]. https://appeears.earthdatacloud.nasa.gov.

Augustin, C., Cihacek, L.J., 2016. Relationships between soil carbon and soil texture in the northern Great Plains. Soil Sci. 181 (8), 386. https://doi.org/10.1097/SS.0000000000000173.

Azene, B., Zhu, R., Pan, K., Sun, X., Nigussie, Y., Gruba, P., Raza, A., Guadie, A., Wu, X., Zhang, L., 2023. Land use change alters phosphatase enzyme activity and phosphatase-harboring microbial abundance in the subalpine ecosystem of southeastern Qinghai-Tibet plateau, China. Ecol. Indic. 153, 110416. https://doi.org/10.1016/j.ecolind.2023.110416.

Baker, N.R., Allison, S.D., 2017. Extracellular enzyme kinetics and thermodynamics along a climate gradient in southern California. Soil Biol. Biochem. 114, 82–92. https://doi.org/10.1016/j.soilbio.2017.07.005.

Balume, I., Agumas, B., Musyoki, M., Marhan, S., Cadisch, G., Rasche, F., 2022. Potential proteolytic enzyme activities modulate archaeal and bacterial nitrifier abundance in soils differing in acidity and organic residue treatment. Appl. Soil Ecol. 169, 104188. https://doi.org/10.1016/j.apsoil.2021.104188.

Bärlocher, F., Porter, C.W., 1986. Digestive enzymes and feeding strategies of three stream invertebrates. J. N. Am. Benthol. Soc. 5 (1), 58–66. https://doi.org/10.2307/1467747.

Barton, K., 2022. MuMIn: Multi-Model Inference. https://CRAN.R-project.org/package=MuMIn.

Bastida, F., Eldridge, D.J., García, C., Kenny Png, G., Bardgett, R.D., Delgado-Baquerizo, M., 2021. Soil microbial diversity–biomass relationships are driven by soil carbon content across global biomes. ISME J. 15 (7), 2081–2091. https://doi.org/10.1038/s41396-021-00906-0.

Bates, D., Mächler, M., Bolker, B., Walker, S., 2015. Fitting linear mixed-effects models using lme4. J. Stat. Softw. 67 (1), 1–48. https://doi.org/10.18637/jss.v067.i01.

Bokulich, N.A., Kaehler, B.D., Rideout, J.R., Dillon, M., Bolyen, E., Knight, R., Huttley, G. A., Gregory Caporaso, J., 2018. Optimizing taxonomic classification of marker-gene amplicon sequences with QIIME 2's q2-feature-classifier plugin. Microbiome 6 (1), 90. https://doi.org/10.1186/s40168-018-0470-z.

Bolyen, E., Rideout, J.R., Dillon, M.R., Bokulich, N.A., Abnet, C.C., Al-Ghalith, G.A., Alexander, H., Alm, E.J., Arumugam, M., Asnicar, F., & others, 2019. Reproducible, interactive, scalable and extensible microbiome data science using QIIME 2. Nat. Biotechnol. 37 (8), 852–857.

Bratbak, G., 1985. Bacterial biovolume and biomass estimations. Appl. Environ. Microbiol. 49 (6), 1488–1493. https://doi.org/10.1128/aem.49.6.1488-1493.1985.

Brown, H.E., Esher, S.K., Alspaugh, J.A., 2019. Chitin: A "hidden figure" in the fungal Cell Wall. In: Latgé, J.-P. (Ed.), The Fungal Cell Wall, 425. Springer International Publishing, pp. 83–111. https://doi.org/10.1007/82_2019_184.

Callahan, B.J., McMurdie, P.J., Rosen, M.J., Han, A.W., Johnson, A.J.A., Holmes, S.P., 2016. DADA2: high-resolution sample inference from Illumina amplicon data. Nat. Methods 13 (7), 581–583. https://doi.org/10.1038/nmeth.3869.

Chantigny, M.H., Harrison-Kirk, T., Curtin, D., Beare, M., 2014. Temperature and duration of extraction affect the biochemical composition of soil water-extractable organic matter. Soil Biol. Biochem. 75, 161–166. https://doi.org/10.1016/j.soilbio.2014.04.011.

Coble, P.G., 1996. Characterization of marine and terrestrial DOM in seawater using excitation-emission matrix spectroscopy. Mar. Chem. 51 (4), 325–346. https://doi.org/10.1016/0304-4203(95)00062-3.

Coleine, C., Selbmann, L., Singh, B.K., Delgado-Baquerizo, M., 2022. The poly-extreme tolerant black yeasts are prevalent under high ultraviolet light and climatic seasonality across soils of global biomes. Environ. Microbiol. 24 (4), 1988–1999. https://doi.org/10.1111/1462-2920.15969.

Conradie, T.A., Jacobs, K., 2021. Distribution patterns of Acidobacteriota in different fynbos soils. PLoS One 16 (3), e0248913. https://doi.org/10.1371/journal.pone.0248913.

Cory, R.M., McKnight, D.M., 2005. Fluorescence spectroscopy reveals ubiquitous presence of oxidized and reduced Quinones in dissolved organic matter. Environ. Sci. Technol. 39 (21), 8142–8149. https://doi.org/10.1021/es0506962.

Cowan, D., Lebre, P., Amon, C., Becker, R., Boga, H., Boulangé, A., Chiyaka, T., Coetzee, T., de Jager, P., Dikinya, O., Eckardt, F., Greve, M., Harris, M., Hopkins, D., Houngnandan, H., Houngnandan, P., Jordaan, K., Kaimoyo, E., Kambura, A., Zeze, A., 2022. Biogeographical survey of soil microbiomes across sub-Saharan Africa: structure, drivers, and predicted climate-driven changes. Microbiome 10 (1), 131. https://doi.org/10.1186/s40168-022-01297-w.

Delgado-Baquerizo, M., Maestre, F.T., Gallardo, A., Bowker, M.A., Wallenstein, M.D., Quero, J.L., Ochoa, V., Gozalo, B., García-Gómez, M., Soliveres, S., García-Palacios, P., Berdugo, M., Valencia, E., Escolar, C., Arredondo, T., Barraza-Zepeda, C., Bran, D., Carreira, J.A., Chaieb, M., Zaady, E., 2013. Decoupling of soil nutrient cycles as a function of aridity in global drylands. Nature 502 (7473), 672–676. https://doi.org/10.1038/nature12670.

Delgado-Baquerizo, M., Maestre, F.T., Reich, P.B., Jeffries, T.C., Gaitan, J.J., Encinar, D., Berdugo, M., Campbell, C.D., Singh, B.K., 2016. Microbial diversity drives multifunctionality in terrestrial ecosystems. Nat. Commun. 7 (1), 10541. https://doi.org/10.1038/ncomms10541.

Delgado-Baquerizo, M., Doulcier, G., Eldridge, D.J., Stouffer, D.B., Maestre, F.T., Wang, J., Powell, J.R., Jeffries, T.C., Singh, B.K., 2020. Increases in aridity lead to drastic shifts in the assembly of dryland complex microbial networks. Land Degrad. Dev. 31 (3), 346–355. https://doi.org/10.1002/ldr.3453.

Dong, L., Li, M.-X., Li, S., Yue, L.-X., Ali, M., Han, J.-R., Lian, W.-H., Hu, C.-J., Lin, Z.-L., Shi, G.-Y., Wang, P.-D., Gao, S.-M., Lian, Z.-H., She, T.-T., Wei, Q.-C., Deng, Q.-Q., Hu, Q., Xiong, J.-L., Liu, Y.-H., Li, W.-J., 2024. Aridity drives the variability of desert soil microbiomes across North-Western China. Sci. Total Environ. 907, 168048. https://doi.org/10.1016/j.scitotenv.2023.168048.

Durán, J., Delgado-Baquerizo, M., Dougill, A.J., Guuroh, R.T., Linstädter, A., Thomas, A. D., Maestre, F.T., 2018. Temperature and aridity regulate spatial variability of soil multifunctionality in drylands across the globe. Ecology 99 (5), 1184–1193. https://doi.org/10.1002/ecy.2199.

Eduardo, N., Florencia, S., Nicolás, P., József, G., 2018. Richness, species composition and functional groups in Agaricomycetes communities along a vegetation and elevational gradient in the Andean Yungas of Argentina. Biodivers. Conserv. 27 (8), 1849–1871. https://doi.org/10.1007/s10531-018-1512-3.

Ekanayaka, A.H., Hyde, K.D., Gentekaki, E., McKenzie, E.H.C., Zhao, Q., Bulgakov, T.S., Camporesi, E., 2019. Preliminary classification of Leotiomycetes. Mycosphere 10 (1), 310–489. https://doi.org/10.5943/mycosphere/10/1/7.

Eslaminejad, P., Heydari, M., Kakhki, F.V., Mirab-balou, M., Omidipour, R., Muñoz-Rojas, M., Lucas-Borja, M.E., 2020. Plant species and season influence soil physicochemical properties and microbial function in a semi-arid woodland ecosystem. Plant Soil 456 (1–2), 43–59. https://doi.org/10.1007/s11104-020-04691-1.

Fierer, N., 2017. Embracing the unknown: disentangling the complexities of the soil microbiome. Nat. Rev. Microbiol. 15 (10), 579–590. https://doi.org/10.1038/nrmicro.2017.87.

Frey, B., Rime, T., Phillips, M., Stierli, B., Hajdas, I., Widmer, F., Hartmann, M., 2016. Microbial diversity in European alpine permafrost and active layers. FEMS Microbiol. Ecol. 92 (3), fiw018. https://doi.org/10.1093/femsec/fiw018.

Friedl, M., Sulla-Menashe, D., 2019. MCD12Q1 MODIS/Terra+aqua land cover type yearly L3 global 500m SIN grid V006 [dataset]. NASA EOSDIS Land Processes Distributed Active Archive Center. https://doi.org/10.5067/MODIS/MCD12Q1.006.

Gee, G.W., Bauder, J.W., 1986. Particle-size analysis. In: Klute, A. (Ed.), Methods of Soil Analysis: Part 1 Physical and Mineralogical Methods, 5. Soil Science Society of America, American Society of Agronomy, pp. 383–411. https://doi.org/10.2136/sssabookser5.1.2ed.c15.

Gessner, M.O., 2005. Ergosterol as a measure of fungal biomass. In: Graça, M.A.S., Bärlocher, F., Gessner, M.O. (Eds.), Methods to Study Litter Decomposition: A Practical Guide. Springer, Netherlands, pp. 189–195. https://doi.org/10.1007/1-4020-3466-0_25.

Gionchetta, G., Oliva, F., Menéndez, M., Lopez Laseras, P., Romaní, A.M., 2019. Key role of streambed moisture and flash storms for microbial resistance and resilience to long-term drought. Freshw. Biol. 64 (2), 306–322. https://doi.org/10.1111/fwb.13218.

Gionchetta, G., Frossard, A., Bañeras, L., Romaní, A.M., 2020. Changes in precipitation patterns: Responses and strategies from streambed sediment and soil microbes. In: Climate Change and Microbial Ecology: Current Research and Future Trends, (Second Edition) (2nd ed. Caister Academic Press, pp. 391–420. https://doi.org/10.21775/9781913652579.

Guber, A., Blagodatskaya, E., Kravchenko, A., 2022. Are enzymes transported in soils by water fluxes? Soil Biol. Biochem. 168, 108633. https://doi.org/10.1016/j.soilbio.2022.108633.

Guo, X., Li, H., Huo, D., Hu, C., Li, R., Zhang, S., Song, L., 2023. Aridity modulates biogeographic distribution and community assembly of cyanobacterial morphotypes in drylands. FEMS Microbiol. Ecol. 99 (6), fiad053. https://doi.org/10.1093/femsec/fiad053.

Hassink, J., 1997. The capacity of soils to preserve organic C and N by their association with clay and silt particles. Plant Soil 191, 77–87. https://doi.org/10.1023/A:1004213929699.

Helms, J.R., Stubbins, A., Ritchie, J.D., Minor, E.C., Kieber, D.J., Mopper, K., 2008. Absorption spectral slopes and slope ratios as indicators of molecular weight, source, and photobleaching of chromophoric dissolved organic matter. Limnol. Oceanogr. 53 (3), 955–969. https://doi.org/10.4319/lo.2008.53.3.0955.

Huguet, A., Vacher, L., Relexans, S., Saubusse, S., Froidefond, J.M., Parlanti, E., 2009. Properties of fluorescent dissolved organic matter in the Gironde estuary. Org. Geochem. 40 (6), 706–719. https://doi.org/10.1016/j.orggeochem.2009.03.002.

Jansson, J.K., Hofmockel, K.S., 2020. Soil microbiomes and climate change. Nat. Rev. Microbiol. 18 (1), 35–46. https://doi.org/10.1038/s41579-019-0265-7.

Johnston, P.R., Quijada, L., Smith, C.A., Baral, H.-O., Hosoya, T., Baschien, C., Pärtel, K., Zhuang, W.-Y., Haelewaters, D., Park, D., Carl, S., López-Giráldez, F., Wang, Z., Townsend, J.P., 2019. A multigene phylogeny toward a new phylogenetic classification of Leotiomycetes. IMA Fungus 10 (1), 1. https://doi.org/10.1186/s43008-019-0002-x.

Kuo, S., 1996. Phosphorus. In: Sparks, D.L., Page, A.L., Helmke, P.A., Loeppert, R.H., Soltanpour, P.N., Tabatabai, M.A., Johnston, C.T., Sumner, M.E. (Eds.), Methods of Soil Analysis, Part 3: Chemical Methods. Soil Science Society of America Inc, pp. 869–919.

Kwok, A.B.C., Wardle, G.M., Greenville, A.C., Dickman, C.R., 2016. Long-term patterns of invertebrate abundance and relationships to environmental factors in arid Australia. Austral Ecol. 41 (5), 480–491. https://doi.org/10.1111/aec.12334.

Lázaro, R., Calvo-Cases, A., Rodriguez-Caballero, E., Arnau-Rosalén, E., Alexander, R., Rubio, C., Cantón, Y., Solé-Benet, A., Puigdefábregas, J., 2022. Biocrusts and catchment asymmetry in Tabernas Desert (Almeria, Spain). Geoderma 406, 115526. https://doi.org/10.1016/j.geoderma.2021.115526.

León-Sobrino, C., Ramond, J.-B., Maggs-Kölling, G., Cowan, D.A., 2019. Nutrient acquisition, rather than stress response over diel cycles, drives microbial transcription in a hyper-arid Namib Desert soil. Front. Microbiol. 10, 1054. https://doi.org/10.3389/fmicb.2019.01054.

Leung, P.M., Bay, S.K., Meier, D.V., Chiri, E., Cowan, D.A., Gillor, O., Woebken, D., Greening, C., 2020. Energetic basis of microbial growth and persistence in desert ecosystems. mSystems 5 (2). https://doi.org/10.1128/msystems.00495-19.

Li, C., Liao, H., Xu, L., Wang, C., He, N., Wang, J., Li, X., 2022. The adjustment of life history strategies drives the ecological adaptations of soil microbiota to aridity. Mol. Ecol. 31 (10), 2920–2934. https://doi.org/10.1111/mec.16445.

Liu, N., Hu, H., Ma, W., Deng, Y., Dimitrov, D., Wang, Q., Shrestha, N., Su, X., Feng, K., Liu, Y., Hao, B., Zhang, X., Feng, X., Wang, Z., 2023. Relationships between soil microbial diversities across an aridity gradient in temperate grasslands. Microb. Ecol. 85 (3), 1013–1027. https://doi.org/10.1007/s00248-022-01997-8.

Liu, W., Zhang, Z., Wan, S., 2009. Predominant role of water in regulating soil and microbial respiration and their responses to climate change in a semiarid grassland. Glob. Chang. Biol. 15 (1), 184–195. https://doi.org/10.1111/j.1365-2486.2008.01728.x.

Liu, Y., He, N., Wen, X., Yu, G., Gao, Y., Jia, Y., 2016. Patterns and regulating mechanisms of soil nitrogen mineralization and temperature sensitivity in Chinese terrestrial ecosystems. Agr. Ecosyst. Environ. 215, 40–46. https://doi.org/10.1016/j.agee.2015.09.012.

Lladó, S., Žifčáková, L., Větrovský, T., Eichlerová, I., Baldrian, P., 2016. Functional screening of abundant bacteria from acidic forest soil indicates the metabolic potential of Acidobacteria subdivision 1 for polysaccharide decomposition. Biol. Fertil. Soils 52 (2), 251–260. https://doi.org/10.1007/s00374-015-1072-6.

Louca, S., Polz, M.F., Mazel, F., Albright, M.B.N., Huber, J.A., O'Connor, M.I., Ackermann, M., Hahn, A.S., Srivastava, D.S., Crowe, S.A., Doebeli, M., Parfrey, L.W., 2018. Function and functional redundancy in microbial systems. Nature Ecology & Evolution 2 (6), 936–943. https://doi.org/10.1038/s41559-018-0519-1.

Luchman, J., 2024. Domir: tools to support relative importance analysis. https://CRAN.R-project.org/package=domir.

Maestre, F.T., Delgado-Baquerizo, M., Jeffries, T.C., Eldridge, D.J., Ochoa, V., Gozalo, B., Quero, J.L., García-Gómez, M., Gallardo, A., Ulrich, W., Bowker, M.A., Arredondo, T., Barraza-Zepeda, C., Bran, D., Florentino, A., Gaitán, J., Gutiérrez, J. R., Huber-Sannwald, E., Jankju, M., Singh, B.K., 2015. Increasing aridity reduces soil microbial diversity and abundance in global drylands. Proc. Natl. Acad. Sci. 112 (51), 15684–15689. https://doi.org/10.1073/pnas.1516684112.

Maier, S., Tamm, A., Wu, D., Caesar, J., Grube, M., Weber, B., 2018. Photoautotrophic organisms control microbial abundance, diversity, and physiology in different types of biological soil crusts. ISME J. 12 (4), 1032–1046. https://doi.org/10.1038/s41396-018-0062-8.

Makhalanyane, T.P., Pointing, S.B., Cowan, D.A., 2014. Lithobionts: Cryptic and refuge niches. In: Cowan, D.A. (Ed.), Antarctic Terrestrial Microbiology. Springer Berlin Heidelberg, pp. 163–179. https://doi.org/10.1007/978-3-642-45213-0_9.

Makhalanyane, T.P., Valverde, A., Gunnigle, E., Frossard, A., Ramond, J.-B., Cowan, D. A., 2015. Microbial ecology of hot desert edaphic systems. FEMS Microbiol. Rev. 39 (2), 203–221. https://doi.org/10.1093/femsre/fuu011.

Marasco, R., Fusi, M., Rolli, E., Ettoumi, B., Tambone, F., Borin, S., Ouzari, H., Boudabous, A., Sorlini, C., Cherif, A., Adani, F., Daffonchio, D., 2021. Aridity modulates belowground bacterial community dynamics in olive tree. Environ. Microbiol. 23 (10), 6275–6291. https://doi.org/10.1111/1462-2920.15764.

Martin, M., 2011. Cutadapt removes adapter sequences from high-throughput sequencing reads. EMBnet.J. 17 (1). https://doi.org/10.14806/ej.17.1.200 article 1.

Matheis, G., Whitaker, J.R., 1984. Modification of proteins by polyphenol oxidase and peroxidase and their products. J. Food Biochem. 8 (3), 137–162. https://doi.org/10.1111/j.1745-4514.1984.tb00322.x.

McHugh, T.A., Compson, Z., Van Gestel, N., Hayer, M., Ballard, L., Haverty, M., Hines, J., Irvine, N., Krassner, D., Lyons, T., Musta, E.J., Schiff, M., Zint, P., Schwartz, E., 2017. Climate controls prokaryotic community composition in desert soils of the southwestern United States. FEMS Microbiol. Ecol. 93 (10). https://doi.org/10.1093/femsec/fix116.

Montgomery, H.J., Monreal, C.M., Young, J.C., Seifert, K.A., 2000. Determinination of soil fungal biomass from soil ergosterol analyses. Soil Biol. Biochem. 32 (8–9), 1207–1217. https://doi.org/10.1016/S0038-0717(00)00037-7.

Morón-Ríos, A., Rodríguez, M.Á., Pérez-Camacho, L., Rebollo, S., 2010. Effects of seasonal grazing and precipitation regime on the soil macroinvertebrates of a Mediterranean old-field. Eur. J. Soil Biol. 46 (2), 91–96. https://doi.org/10.1016/j.ejsobi.2009.12.008.

Mugnai, G., Pinchuk, I., Borruso, L., Tiziani, R., Sannino, C., Canini, F., Turchetti, B., Mimmo, T., Zucconi, L., Buzzini, P., 2024. The hidden network of biocrust successional stages in the high Arctic: revealing abiotic and biotic factors shaping microbial and metazoan communities. Sci. Total Environ. 926, 171786. https://doi.org/10.1016/j.scitotenv.2024.171786.

Naimi, B., Hamm, N. a s, Groen, T.A., Skidmore, A.K., Toxopeus, A.G., 2014. Where is positional uncertainty a problem for species distribution modelling? Ecography 37, 191–203. https://doi.org/10.1111/j.1600-0587.2013.00205.x.

Nannipieri, P., Ceccanti, B., Bianchi, D., 1988. Characterization of humus-phosphatase complexes extracted from soil. Soil Biol. Biochem. 20 (5), 683–691. https://doi.org/10.1016/0038-0717(88)90153-8.

Nannipieri, P., Ascher, J., Ceccherini, M.T., Landi, L., Pietramellara, G., Renella, G., 2003. Microbial diversity and soil functions. Eur. J. Soil Sci. 54 (4), 655–670. https://doi.org/10.1046/j.1351-0754.2003.0556.x.

Neilson, J.W., Quade, J., Ortiz, M., Nelson, W.M., Legatzki, A., Tian, F., LaComb, M., Betancourt, J.L., Wing, R.A., Soderlund, C.A., Maier, R.M., 2012. Life at the hyperarid margin: novel bacterial diversity in arid soils of the Atacama Desert, Chile. Extremophiles 16 (3), 553–566. https://doi.org/10.1007/s00792-012-0454-z.

Neilson, J.W., Califf, K., Cardona, C., Copeland, A., Van Treuren, W., Josephson, K.L., Knight, R., Gilbert, J.A., Quade, J., Caporaso, J.G., Maier, R.M., 2017. Significant impacts of increasing aridity on the arid soil microbiome. mSystems 2 (3). https://doi.org/10.1128/mSystems.00195-16 e00195-16.

Nouhra, E., Soteras, M.F., Pastor, N., Geml, J., 2018. Richness, species composition and functional groups in Agaricomycetes communities along a vegetation and elevational gradient in the Andean Yungas of Argentina. Biodivers. Conserv. 27 (8), 1849–1871. https://doi.org/10.1007/s10531-018-1512-3.

Oksanen, J., Simpson, G.L., Blanchet, F.G., Kindt, R., Legendre, P., Minchin, P.R., O'Hara, R.B., Solymos, P., Stevens, M.H.H., Szoecs, E., Wagner, H., Barbour, M., Bedward, M., Bolker, B., Borcard, D., Carvalho, G., Chirico, M., Caceres, M.D., Durand, S., Weedon, J., 2022. Vegan: community ecology package. https://CRAN.R-project.org/package=vegan.

Parlanti, E., Wörz, K., Geoffroy, L., Lamotte, M., 2000. Dissolved organic matter fluorescence spectroscopy as a tool to estimate biological activity in a coastal zone submitted to anthropogenic inputs. Org. Geochem. 31 (12), 1765–1781. https://doi.org/10.1016/S0146-6380(00)00124-8.

Pedregosa, F., Varoquaux, G., Gramfort, A., Michel, V., Thirion, B., Grisel, O., Blondel, M., Prettenhofer, P., Weiss, R., Dubourg, V., others, 2011. Scikit-learn: machine learning in Python. J. Mach. Learn. Res. 12, 2825–2830.

Puissant, J., Jones, B., Goodall, T., Mang, D., Blaud, A., Gweon, H.S., Malik, A., Jones, D. L., Clark, I.M., Hirsch, P.R., Griffiths, R., 2019. The pH optimum of soil exoenzymes adapt to long term changes in soil pH. Soil Biol. Biochem. 138, 107601. https://doi.org/10.1016/j.soilbio.2019.107601.

Quast, C., Pruesse, E., Yilmaz, P., Gerken, J., Schweer, T., Yarza, P., Peplies, J., Glöckner, F.O., 2013. The SILVA ribosomal RNA gene database project: improved data processing and web-based tools. Nucleic Acids Res. 41 (D1), D590–D596. https://doi.org/10.1093/nar/gks1219.

R Core Team, 2021. R: A Language and Environment for Statistical Computing. R Foundation for Statistical Computing. https://www.R-project.org/.

Rakhsh, F., Golchin, A., Beheshti Al Agha, A., Nelson, P.N., 2020. Mineralization of organic carbon and formation of microbial biomass in soil: effects of clay content and composition and the mechanisms involved. Soil Biol. Biochem. 151, 108036. https://doi.org/10.1016/j.soilbio.2020.108036.

Salazar, S., Sánchez, L.E., Alvarez, J., Valverde, A., Galindo, P., Igual, J.M., Peix, A., Santa-Regina, I., 2011. Correlation among soil enzyme activities under different forest system management practices. Ecol. Eng. 37 (8), 1123–1131. https://doi.org/10.1016/j.ecoleng.2011.02.007.

Schimel, J. P. (2018). Life in dry soils: effects of drought on soil microbial communities and processes. In *annual review of ecology, evolution, and systematics* (Vol. 49, issue volume 49, 2018, pp. 409–432). Annual reviews. doi:https://doi.org/10.1146/annurev-ecolsys-110617-062614.

Schimel, J.P., Balser, T.C., Wallenstein, M., 2007. Microbial stress-response physiology and its implications for ecosystem function. Ecology 88 (6), 1386–1394. https://doi.org/10.1890/06-0219.

Song, H.-K., Shi, Y., Yang, T., Chu, H., He, J.-S., Kim, H., Jablonski, P., Adams, J.M., 2019. Environmental filtering of bacterial functional diversity along an aridity gradient. Sci. Rep. 9 (1), 866. https://doi.org/10.1038/s41598-018-37565-9.

Starke, R., Capek, P., Morais, D., Callister, S.J., Jehmlich, N., 2020. The total microbiome functions in bacteria and fungi. J. Proteome 213, 103623. https://doi.org/10.1016/j.jprot.2019.103623.

Stock, S.C., Köster, M., Dippold, M.A., Nájera, F., Matus, F., Merino, C., Boy, J., Spielvogel, S., Gorbushina, A., Kuzyakov, Y., 2019. Environmental drivers and stoichiometric constraints on enzyme activities in soils from rhizosphere to continental scale. Geoderma 337, 973–982. https://doi.org/10.1016/j.geoderma.2018.10.030.

Sulla-Menashe, D., Friedl, M.A., 2018. User Guide to Collection 6 MODIS Land Cover (MCD12Q1 and MCD12C1) Product.

Tale, K.S., Ingole, D.S., 2015. A Review on Role of Physico-Chemical Properties in Soil Quality.

Tan, X., Nie, Y., Ma, X., Guo, Z., Liu, Y., Tian, H., Megharaj, M., Shen, W., He, W., 2021. Soil chemical properties rather than the abundance of active and potentially active microorganisms control soil enzyme kinetics. Sci. Total Environ. 770, 144500. https://doi.org/10.1016/j.scitotenv.2020.144500.

Theil-Nielsen, J., Søndergaard, M., 1998. Bacterial carbon biomass calculated from biovolumes. Arch. Hydrobiol. 195–207. https://doi.org/10.1127/archiv-hydrobiol/141/1998/195.

Theuerl, S., Dörr, N., Guggenberger, G., Langer, U., Kaiser, K., Lamersdorf, N., Buscot, F., 2010. Response of recalcitrant soil substances to reduced N deposition in a spruce forest soil: integrating laccase-encoding genes and lignin decomposition. FEMS Microbiol. Ecol. 73 (1), 166–177. https://doi.org/10.1111/j.1574-6941.2010.00877.x.

Trabucco, A., Zomer, R., 2022. *Global Aridity Index and Potential Evapotranspiration (ET0) Climate Database v3* (Version 4) [Dataset]. https://doi.org/10.6084/m9.figshare.7504448.v4.

Védère, C., Lebrun, M., Honvault, N., Aubertin, M.-L., Girardin, C., Garnier, P., Dignac, M.-F., Houben, D., Rumpel, C., 2022. How does soil water status influence the fate of soil organic matter? A review of processes across scales. Earth Sci. Rev. 234, 104214. https://doi.org/10.1016/j.earscirev.2022.104214.

Voeten, C.C., 2023. Buildmer: stepwise elimination and term reordering for mixed-effects regression. https://CRAN.R-project.org/package=buildmer.

Walthert, L., Graf, U., Kammer, A., Luster, J., Pezzotta, D., Zimmermann, S., Hagedorn, F., 2010. Determination of organic and inorganic carbon, $\delta^{13}$ C, and nitrogen in soils containing carbonates after acid fumigation with HCl. J. Plant Nutr. Soil Sci. 173 (2), 207–216. https://doi.org/10.1002/jpln.200900158.

Wang, J., Yuan, Y., Zhang, M., Dai, X., He, H., Li, H., Li, Y., 2020. Impact of degradation and restoration on soil fungi and extracellular enzyme activity in alpine rangelands on the Tibetan plateau. Arch. Agron. Soil Sci. 67 (14), 1917–1929. https://doi.org/10.1080/03650340.2020.1818071.

Wang, S., Zuo, X., Awada, T., Medima-Roldán, E., Feng, K., Yue, P., Lian, J., Zhao, S., Cheng, H., 2021. Changes of soil bacterial and fungal community structure along a natural aridity gradient in desert grassland ecosystems, Inner Mongolia. CATENA 205, 105470. https://doi.org/10.1016/j.catena.2021.105470.

Wang, X., Zeng, J., Chen, F., Wang, Z., Liu, H., Zhang, Q., Liu, W., Wang, W., Guo, Y., Niu, Y., Yuan, L., Ren, C., Yang, G., Zhong, Z., Han, X., 2024. Aridity shapes distinct biogeographic and assembly patterns of forest soil bacterial and fungal communities at the regional scale. Sci. Total Environ. 948, 174812. https://doi.org/10.1016/j.scitotenv.2024.174812.

Yang, T., Li, X., Hu, B., Wei, D., Wang, Z., Bao, W., 2022. Soil microbial biomass and community composition along a latitudinal gradient in the arid valleys of Southwest China. Geoderma 413, 115750. https://doi.org/10.1016/j.geoderma.2022.115750.

Zang, X., Liu, M., Wang, H., Fan, Y., Zhang, H., Liu, J., Xing, E., Xu, X., Li, H., 2017. The distribution of active β-glucosidase-producing microbial communities in composting. Can. J. Microbiol. 63 (12), 998–1008. https://doi.org/10.1139/cjm-2017-0368.

Zárate-Valdez, J.L., Zasoski, R.J., Läuchli, A.E., 2006. Short-term effects of moisture content on soil solutions pH and soil eh. Soil Sci. 171 (5), 423. https://doi.org/10.1097/01.ss.0000222887.13383.08.

Zhang, Z., Zhao, G., Cong, M., Tariq, A., Lu, Y., Zeng, F., 2024. Metagenomic insights into microbial diversity and carbon cycling related genes along the elevational gradient in an arid mountain ecosystem. Pedosphere, S1002016023001352. https://doi.org/10.1016/j.pedsph.2023.12.012.

Zomer, R.J., Xu, J., Trabucco, A., 2022. Version 3 of the global aridity index and potential evapotranspiration database. Scientific Data 9 (1), 409. https://doi.org/10.1038/s41597-022-01493-1.

Zuccarini, P., Sardans, J., Asensio, L., Peñuelas, J., 2023. Altered activities of extracellular soil enzymes by the interacting global environmental changes. Glob. Chang. Biol. 29 (8), 2067–2091. https://doi.org/10.1111/gcb.16604.